Journal of Mining and Environment (JME), Vol. 14, No. 3, 2023, 839-851

Shahrood University of Technology

Journal of Mining and Environment (JME)

Journal homepage: www.jme.shahroodut.ac.ir

Iranian Society of Mining Engineering (IRSME)

The Efficiency of Clay-Based Adsorbent in Fluoride Removal from Groundwater: Adsorption Process

Muhizi Patrick

Department of Civil Engineering, UIE Chandigarh University, Mohali, India

Article Info

Received 8 April 2023
Received in Revised form 7 June 2023
Accepted 16 June 2023
Published online 16 June 2023

DOI:10.22044/jme.2023.12933.2348

Keywords

Adsorbent
Ceramic clay
Drinking water
Fluoride removal
Remediation technology

Abstract

Excessive amounts of fluoride present in underground water sources are a major health concern worldwide. This study presents a new way to address the global health issue of high fluoride concentrations in groundwater using the abundantly available and cost-effective adsorbent material activated kaolinite clay "WR@KN". The physical and chemical activation methods are employed to enhance its adsorption capacity. The optimum conditions for fluoride removal are determined through batch adsorption experiments, with a maximum adsorption capacity of 0.745 mg/g at pH 6, a particle size of 10 µm, a mixing speed of 210 rpm, a temperature of 24 °C, an initial fluoride concentration of 5.5 mg/L, a dose of 0.7 g activated WR@KN, and a contact period of 240 minutes. WR@KN successfully removes fluoride ions from 5.5 to 0.28 mg/L. The Langmuir isotherm model is found to be the most suitable for describing the adsorption behavior of fluoride on the WR@KN surface with an R2 of 0.99984. The adsorption kinetic modeling shows that the pseudo-second-order model is the best fit with 0.754 mg/g, indicating that the fluoride adsorption process is chemisorption. The exothermic nature of the fluoride adsorption process is confirmed by a negative value of ΔH° (-77.08). The regenerated WR@KN adsorbent could remove fluoride effectively for the first four cycles but its performance deteriorated in the subsequent cycles. Increasing the ionic strength enhances the fluoride removal efficiency. Overall, the results suggest that the WR@KN adsorbent can be a promising material for cost-effective fluoride removal from groundwater.

1. Introduction

Fluoride is the anion of fluorine, which is widely distributed in various geological environments, and is the thirteenth most abundant element in the Earth's crust [1]. Fluorine, being a potent oxidant, naturally exists as the fluoride ion in various minerals including fluorite, sellaite, and apatite, and enters groundwater and surface water through an ion exchange between the fluoride ions in the minerals and the hydroxide ions in the water [2]. In the recent times, excess fluoride has been identified in agricultural and industrial wastewater due to human activities such as aluminum smelting, coal burning, semi-conductor manufacturing, and phosphate fertilizer production [3]. Although fluoride is necessary for human health by strengthening teeth and bones, prolonged ingestion of water with high fluoride concentrations has different drawbacks such as dental fluorosis, skeletal fluorosis, thyroid hormones, Alzheimer's disease, hypertension, and reduced testosterone levels causing infertility [4–8]. The concentration of fluoride in drinking water is considered a human health concern if it exceeds the permissible range of 0.5-1.5 mg/L, as set by the World Health Organization (WHO) [9]. Globally, an estimated 200 million people in 35 different countries suffer from dangerous fluoride concentrations beyond the recommended limits in groundwater and surface water, with India, China, Pakistan, Afghanistan, Brazil, South Africa, Malawi, and Ethiopia being the most affected by fluorosis [10–12]. Therefore, several methods are continually being developed to reduce the high concentrations of fluoride found in

✉ *Corresponding author: mupax49@gmail.com (M. Patrick)*

water to the permissible level for drinking water, as discussed in our previous work [13].

Presently, the de-fluoridation techniques that have been developed such as chemical coagulation and precipitation exhibit elevated efficacy in eliminating fluoride from both groundwater and surface water [1, 14–17]. However, additional treatment is required to bring the effluent within permissible limits [18]. Moreover, these approaches necessitate the usage of expensive and abundant chemicals, resulting in the generation of copious amounts of sludge that must be appropriately managed before disposal [15]. Alternative technologies such as electrodialysis, electrocoagulation, ion exchange, nanofiltration, and reverse osmosis have demonstrated high effectiveness in eliminating fluoride from the water up to the acceptable range for drinking water [19–21]. Nevertheless, these methods are costly and necessitate the engagement of skilled operators [22]. Of all the techniques that have been developed, the adsorption process is considered to be economically feasible, environmentally benign, convenient, and transportable, and can be applied in domestic [23].

Natural adsorbents, including clay, zeolite, soil, lignite, and others, synthetic adsorbents such as activated carbon, and bioadsorbents, like agricultural waste, household waste, and microorganisms have recently exhibited high adsorption capacities for eliminating fluoride [24]. Employing low-cost natural adsorbents such as clay-based materials is one means of significantly reducing the costs associated with the adsorption process, as these adsorbents are abundantly available in nature and environmentally friendly [25]. Generally, clay-based adsorbents are advantageous in water treatment processes because they contain metal atoms such as aluminum, iron, and silicon. that are electrostatically charged or in various stages of oxidation [26]. The positive charge of the active site on the surface of clay-based adsorbents, when the pH is below their pHpzc (pH at point of zero charge) may explain their strong affinity for adsorbing negative ions [27]. These properties allow for physical and chemical interactions with fluoride, resulting in fluoride adhesion to the adsorbent's surface, which increases fluoride removal efficiency [28]. Algerian natural clay (kaolinite) demonstrated a high adsorption capacity of 0.48 mg/g, which was equivalent to the acceptable level of drinking water when utilized as an adsorbent in an adsorption process to remove 5 mg/L fluoride concentrations from groundwater [29]. Furthermore, Diop et al. [25] utilized two types of clays, montmorillonite KSF, and montmorillonite K10, as adsorbents in a de-fluoridation process from water containing 4.50 mg/L fluoride concentration and discovered that these clays have adsorption capacities of 0.298 mg/g and 0.532 mg/g, respectively. Activating WR@KN may also enhance the adsorption capacity, creating more active sites on the adsorbent surface that encourage physical and chemical interactions with fluoride ions, resulting in further improvement of the adsorption capacity. Hence, developing an ecologically favorable, affordable, and efficiently activated WR@KN adsorbent may prove beneficial for fluoride removal. This research work contributes valuable insights, characterizes a new adsorbent from natural-based material, determines optimal operating conditions, and offers practical advantages in terms of cost-effectiveness and potential long-term performance, making it a significant advancement compared to previous works in the field of fluoride removal from groundwater.

In the present investigation, physical and chemical activation techniques were employed to heighten the adsorption capacity of WR@KN. The characterization of the WR@KN was conducted using Fourier-transform infrared spectroscopy (FTIR), scanning electron microscopy (SEM), and X-ray diffraction (XRD). The objective of this research work was to assess the adsorption efficiency of the WR@KN adsorbent in batch mode for the elimination of fluoride. To accomplish this, we optimized various factors affecting the adsorption process such as pH, contact time, temperature, mixing, initial concentration (C_i), size, and adsorbent dosage. The adsorption isotherm and adsorption kinetics were utilized to scrutinize the mechanism of the WR@KN in fluoride adsorption. Additionally, the WR@KN's regeneration capability after the adsorption process was examined to reuse it for de-fluoridation.

2. Materials and Methods

2.1. Materials

All the chemicals used in this study including sodium hydroxide, hydrochloric acid, sodium fluoride, potassium chloride, sodium 2-(parasulfophenylazo)-1,8-dihydroxy-3,6-napthalene disulfonate, and zirconyl chloride octahydrate were obtained from the laboratories of Chandigarh University (Research and

Environmental Labs). These reagents were of analytical grade purity.

2.2. Preparation of adsorbent

The kaolinite in the form of white rocks was obtained from local potters in Kharar, Mohali, Punjab State, India. The white rocks were crushed and sieved to obtain small particles of diameter less than 2 µm. To remove any physical impurities, it was washed with pure water and then washed three times with distilled water. Next, it was dried for 3 hours at 110 °C in a universal oven. The dried clay was soaked in 0.1 N NaOH solution for an hour and then rewashed with distilled water while maintaining a neutral pH using 0.1 N HCl. The clay was then dried for another 3 hours at 110 °C in a hot air oven and ground using a mortar and pestle. The resulting powder was fired in a muffle furnace under anoxic conditions at different temperatures (300, 600, and 800 °C) for 6 hours. The material was allowed to cool for 24 hours in the muffle furnace, then pulverized using a mortar. Finally, the kaolinite clay was stored in plastic bags with the notation WR@KN.

2.3. Experimental setup

A stock solution of fluoride water was produced by dissolving 0.11 g of NaF in 1 L of distilled water. A standard solution with a concentration of 10 ppm was prepared by diluting a portion of the stock solution in a beaker of 100 mL. The appropriate working C_i for the experiment was achieved by diluting the standard solution using the dilution formula. The fluoride was removed from the water through adsorption using activated WR@KN, with the process conducted on a batch scale under room temperature (24 °C). Solutions with varying C_i and dosages of WR@KN were added to conical flasks and stirred at 150 rpm for 120 min on a hot plate with a varying temperature range until adsorption equilibrium was reached. After sedimentation, the solutions were filtered using 90 mmφ Whatman filter paper, and the final fluoride concentration was determined using a UV spectrophotometer. The quantities of fluoride that were adsorbed by the WR@KN were computed utilizing Eq. (1) and Eq. (2), for the purpose of determining the proportion of fluoride elimination expressed as (%F). To evaluate the kinetic data of the de-fluoridation two kinetic models, pseudo-first-order (PFO) Eq. (3), and pseudo-second-order (PSO) Eq. (4) were examined [1, 30]. For the adsorption isotherm model Freundlich Eq. (5), and Langmuir Eq. (6) was studied [29, 30]. The thermodynamic parameter was obtained from Eq. (7). Top of From Bottom of From:

$$qe = \frac{(C_i - C_f) \times V}{m} \quad (1)$$

$$(\%F) = \frac{(C_i - C_f) \times 100}{C_i} \quad (2)$$

$$log(q_e - q_t) = log\ q_e - \frac{k_1 t}{2.303} \quad (3)$$

$$\frac{t}{q_t} = \frac{1}{k_2 q_e^2} + \frac{1}{q_t} \quad (4)$$

$$log\ q_e = \log K_f + \left(\frac{1}{n}\right) \log C_f \quad (5)$$

$$\frac{C_f}{q_e} = \frac{1}{K_L q_{max}} + \frac{C_f}{q_{max}} \quad (6)$$

$$Log(aq_e / C_e) = \left(\frac{\Delta S^{\circ}}{2.303R}\right) + \left(-\frac{\Delta H^{\circ}}{2.303RT}\right) \quad (7)$$

where qe is the amount of F adsorbed at equilibrium, (mg/g) C_i and C_f (both in mg/L) are the initial and final fluoride concentrations respectively, V (L) is the volume of the aqueous solution, and m (g) is the mass of the adsorbent, k_1 is the pseudo-first-order adsorption rate constant (min^{-1}), k_2 (g/mg min) represents the rate constant for the second-order model, n is the adsorption intensity constant, K_f is the Freundlich adsorption constant, q_{max} represents the Langmuir monolayer adsorption capacity (mg/g), and K_L is the Langmuir constant representing the affinity of binding sites (L/mg), a represents the dose (g/L), ΔS° represents the entropy change, R represents the gas constant (8.314 J/mol/K), ΔH° represents the enthalpy change, T represents temperature, and ΔG° represents the Gibbs free energy change.

2.4. Characterization

Four specimens of adsorbent, namely, raw WR@KN, WR@KN washed with acid/base, activated WR@KN, and WR@KN after F adsorption, underwent physical and chemical analyses to investigate the transformation incurred during the activation process. The surface morphology of the WR@KN was examined using SEM; JSM-IT500 at accelerating voltages of 10.0 and 15.0 kV and diverse magnifications ranging from 250 to 1500. The crystalline structure of the WR@KN was studied via XRD, D8 ADVANCE ECHO. The FTIR analysis was conducted to detect any modification of the functional groups involved

in the adsorption process. The pH was measured using a pH-meter (LMPH12), and the pHpzc was determined as the point at which the curve of ΔpH intersects the line of pH initial. The concentration of fluoride in water was measured using UV-VIS double beam spectrophotometer reagent S (SPANDS method).

3. Results and Discussion

3.1. Adsorbent characterization

3.1.1. FTIR

The alteration in peak during WR@KN sample activation was determined using (FTIR) analysis, as presented in **Figure 1a**. Each bond exhibits a distinct vibration frequency characteristic. The valence vibration between 3500 and 3750 cm^{-1} represents the hydroxyl (OH) groups. The Si-O stretching vibrations band is between 1500 and 500 cm^{-1}, which can also be attributed to the vibrational deformation of Si-O-Al and Al-OH-Al, representing the peaks of kaolinite clay [29]. After the acid/base wash, the peaks of kaolinite increased due to the neutralization of alkalinity and the disappearance of some impurities, as observed from the FTIR spectra analysis. Firing the sample at 800 °C increased peak height and sharpened the silica peak, owing to the elimination of remaining impurities. Removal of moisture contents occurred at 300 °C, whereas burning of carbonate materials occurred at 600 °C. At 800 °C, all impurities were burnt, and WR@KN was activated. After fluoride adsorption, the intensity of the silica peak decreased compared to that of activated WR@KN due to the occupancy of fluoride ions on all active sites. The results demonstrate that fluoride ions associated with the adsorbent's surfaces reduce the transmittance of the silica peak by occupying the adsorption sites, as reported by Gasparotto et al. [4]. Furthermore, the intensity of the hydroxyl group shifted to stretching vibrations ranging between 3000 and 3500 cm^{-1}, the observed peaks are attributed to fluoride adsorption on the hydroxyl site. Based on these findings, fluoride interacts with the -OH and –NH functional groups present on the WR@KN's surface. This shifting of the hydroxyl site was also reported in the study conducted by Mondal et al. [30].

3.1.2. XRD

XRD was used to investigate changes in the crystalline structure of WR@KN samples during activation. It was conducted with a scanning rate of 1° min-1 and a step size of 0.05°, covering a 2Θ range of 10-80°. In the raw WR@KN sample, the peaks were reduced **Figure 1b**. However, treatment with acid/base increased the peak of silica and improved the crystalline structure by neutralizing alkalinity and eliminating impurities. Heating at 800 °C further improved the crystallinity by removing the remaining impurities and purifying the WR@KN. The XRD analysis also showed that the peak of silica declined in the post-adsorption sample, indicating that impurities from fluoride-containing water had attached to the adsorbent surface. Similar observations were reported by Saikia and Goswamee [31] during the activation process of ceramic membranes from potters.

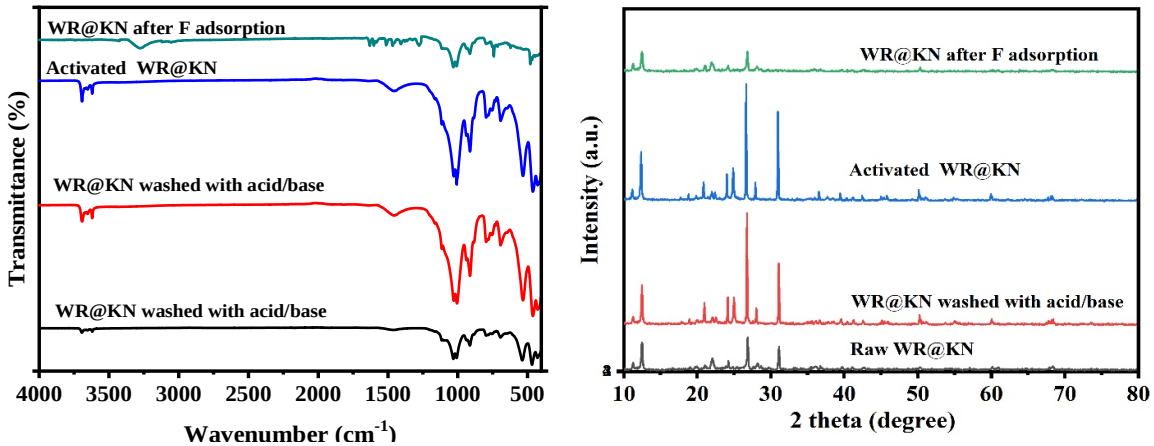

Figure 1. a) FTIR graph; b) XRD graph.

3.1.3. SEM

The activation process of WR@KN was investigated using SEM analysis to visualize the changes in the pore structure. SEM images of various WR@KN samples are presented in **Figure 2**, with sizes ranging from 10 to 100 µm. The results indicate that washing the raw WR@KN with acid/base solutions revealed the pores, as the alkalinity was neutralized, removing impurities on the WR@KN surface. Heating the WR@KN to 800 °C increased pore size and visibility due to the burning off of all impurities, resulting in purified WR@KN. Interestingly, SEM analysis of the WR@KN after adsorption demonstrated a significant decrease in pore size with some pores becoming invisible. This decrease in pore size is attributed to the attraction of impurities (fluoride) to the surface of the adsorbent. Recent studies have confirmed these changes in the adsorbent surface during the activation process [10, 32]. Overall, activated WR@KN offers a higher specific surface area and more active sites than raw WR@KN, making it a promising material for various applications.

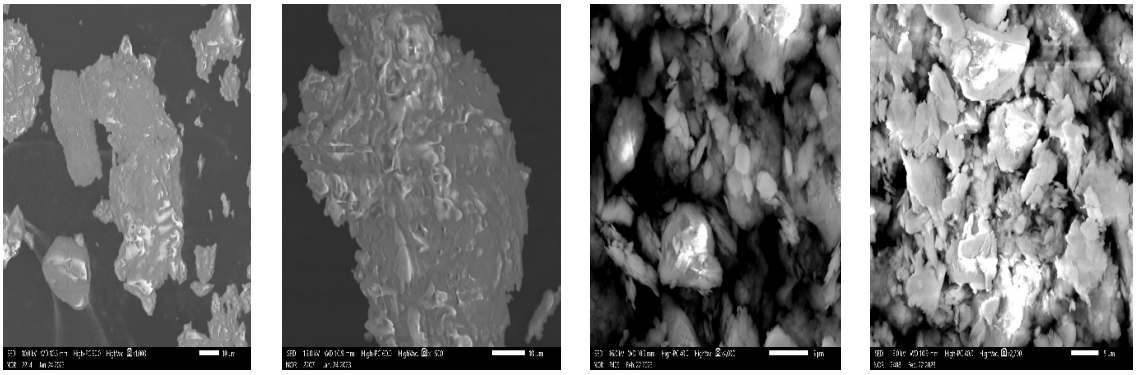

(a) **(b)** **(c)** **(d)**

Figure 2. SEM image (a) raw WR@KN; (b) acid/base wash WR@KN; (c) activated WR@KN, and (d) WR@KN after adsorption.

Table 1. Element of WR@KN (EDS).

Element	O	Mg	Al	Si	K	Ca	Total
Mass (%)	51.79	1.43	16.01	26.62	1.63	2.52	100

3.2. Factor optimization

3.2.1. Effect of pH

Variation of initial pH between 2 and 8 was employed to investigate the impact of pH on fluoride removal in the adsorption process using WR@KN as the adsorbent by maintaining other parameters constant. Results reveal a steep increase in adsorption capacity as pH rises from 4 to 6, corresponding to 0.266 and 0.496 mg/g, respectively (**Figure 3a).** The reduced adsorption capacity of fluoride at pH below 6 may be attributed to the competition between adsorption behavior and hydrofluoric acid production. This competition may limit the available binding sites on the adsorbent surface, leading to reduced fluoride removal. This finding is consistent with a study done by Ayalew [33], which reported a similar correlation between increasing solution pH and adsorption capacity. Furthermore, the results indicated that fluoride removal significantly decreased beyond pH 6, which can be attributed to the pHpzc (point of zero charge) of the WR@KN adsorbent, which was measured to be 6.7 (**Figure 3b)**. Above the pHpzc, the surface of the adsorbent becomes negatively charged, primarily due to hydroxyl ions (OH^-). This negative charge leads to electrostatic repulsion between the negatively charged surface and the fluoride ions, thereby hindering their adsorption. Additionally, the presence of fewer positive ions at higher pH levels reduces the attractive forces responsible for fluoride ion binding. Jeyaseelan et al. [10] also reported similar interactions.

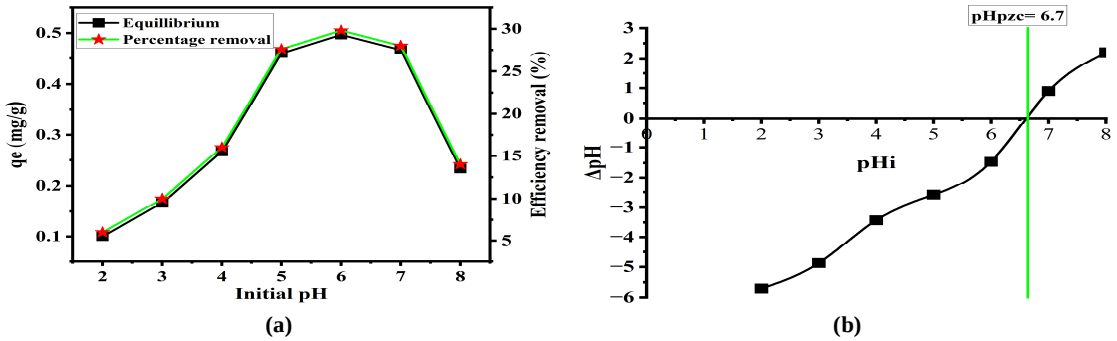

Figure 3. a) Effect of pH on F adsorption; b) pHpzc of adsorbent.

3.2.2. Effect of size

The impact of particle size on the adsorption of fluoride was scrutinized through the utilization of variable particle sizes spanning from 10-100 µm while preserving a pH of 6 that was optimized. The findings presented in **Figure 4a** reveal that by diminishing the particle size from 50 to 10 µm, the efficacy of fluoride removal was heightened by 12%, equating to an increase in adsorption capacity from 0.433 to 0.696 mg/g. The observed increase in fluoride removal efficiency with smaller particle sizes can be attributed to the greater surface area available for adsorption. As the particle size decreases, the total surface area of the adsorbent increases. This larger surface area provides more active sites for fluoride ions to bind to, leading to a higher adsorption capacity. Ghouti and Absi [34] corroborate that adsorption proficiency is contingent on the dimensions of the adsorbent particles and that a decrease in particle size augments adsorption efficiency. Nonetheless, it can be inferred that a decline in the particle size of the adsorbent would enhance the binding surface area.

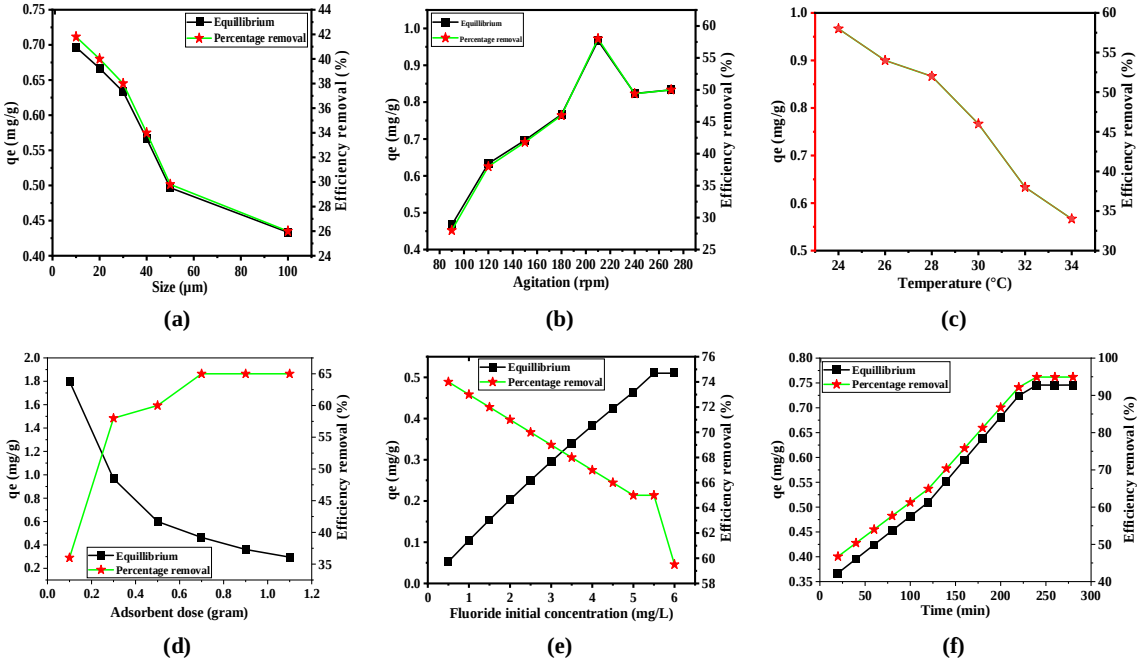

Figure 4. Effect of factors on F adsorption; a) Size, b) Agitation, c) Temperature, d) Dose, e) Initial concentration, f) Time.

3.2.3. Effect of mixing

The impact of variation in mixing velocity on the effectiveness of fluoride elimination using WR@KN has been investigated. The experimentation involved manipulating the mixing speed within the range of 90 to 240 rpm at optimal

factors. The outcomes demonstrate that the efficacy of fluoride removal was 41.8% at 150 rpm and elevated to 50% at 210 rpm, as illustrated in **Figure 4b**. The efficacy of fluoride removal is diminished at low mixing speeds and escalates as the mixing velocity is increased up to 210 rpm. At 240 rpm, it declines to 49.4%, then re-increase to 50% at 270 rpm, where it becomes steady. The escalation in fluoride removal efficacy with an increase in mixing velocity is due to the fact that mixing amplifies turbulence and diminishes the thickness of the boundary layer encircling the adsorbent, thereby allowing a heightened mass transfer between the adsorbent and adsorbate. The marginal increment at 240 rpm is caused by the dissociation of weakly-bonded fluoride from the adsorbent surfaces due to extreme mixing beyond the equilibrium velocity, however, it reverts to 50% removal efficiency at 270 rpm and remains consistent. The identical mixing effect in the adsorption process was confirmed by Mahdi and Jaafar [35].

3.2.4. Effect of temperature

The impact of temperature on the efficiency of fluoride removal during the adsorption process was investigated within a temperature range of 24-34 °C, under optimal conditions. The results indicate that the fluoride removal efficiency decreased from 58% at 24 °C to 52% at 34 °C, which is equivalent to 0.966 to 0.566 mg/g, as shown in **Figure 4c**. This decrease in adsorption capacity can be attributed to the increased deprotonation or hydroxylation of the adsorbent surface, leading to negatively charged adsorbent surfaces that repel fluoride ions electrostatically [36]. It can be inferred from these findings that the adsorption process is exothermic, as the attractive forces acting on the surface of the adsorbent decrease during adsorption, resulting in a drop in the adsorbent's surface energy, which is released as heat [37, 38]. In contrast, Ayalew [33] reported that the adsorption process is endothermic because increasing the temperature increased fluoride removal efficiency.

3.2.5. Effect of dosage

The adsorption procedure was carried out to assess the impact of varying doses, spanning from 0.1 to 1.1 g per 100 mL, on the elimination of fluoride using WR@KN under conditions that have been optimized. According to the findings displayed in **Figure 4d**, it can be observed that when the adsorbent dose was raised from 0.3 g to 0.7 g, the efficacy of fluoride removal increased from 58% to 65%. This can be attributed to the fact that the increase in adsorbent dose leads to a rise in the number of active sites on the adsorbent surface, which consequently results in more effective de-fluoridation [36]. Subsequently, when the adsorbent dose was raised to 1.1 g, the removal efficiency remained stable, indicating that the equilibrium had been achieved. Recent studies have also reported similar observations regarding the impact of varying adsorbent doses on fluoride removal [1, 2].

3.2.6. Effect of fluoride concentration

The impact of the C_i in the adsorption procedure was assessed through the utilization of various concentrations of fluoride ranging from 0.5 to 6 mg/L, under optimized conditions. As presented in **Figure 4e**, the adsorption capacity is influenced by the C_i. An elevation in the C_i from 0.5 to 5.5 mg/L results in a decrease in the removal efficiency and an increase in the adsorption capacity from 0.052 to 0.51 mg/g, respectively, which subsequently stabilizes at 6 mg/L. This is attributed to the availability of a greater number of functional groups on the surface of the adsorbent at lower fluoride concentrations, resulting in enhanced de-fluoridation efficacy. However, as the fluoride concentration is increased, this effectiveness is diminished [39]. Furthermore, the adsorption capacity rises with an increase in C_i, since more fluoride ions surround the active sites of WR@KN, leading to saturation. This implies that a rise in the C_i results in an elevation in the driving force for mass transfer, leading to higher adsorption capacity. This is consistent with a previous finding by Ayalew [33].

3.2.7. Effect of time

The present study aimed to investigate the impact of contact duration on fluoride adsorption using WR@KN as an adsorbent. Several contact times ranging from 20 to 280 minutes were examined while controlling optimized factors. According to the results presented in **Figure 4f**, rapid adsorption of fluoride ions was observed during the initial 20 minutes of contact time, resulting in an efficient removal rate of 46.72%. Subsequently, the fluoride removal rate increased gradually up to 240 minutes and then stabilized for the remaining 40 minutes. This trend may be attributed to the availability of more vacant and active sites on the adsorbent's surface during the initial contact time. After a certain duration, the adsorbent surface may have been saturated, and the presence of fluoride ions may have caused a reduction in the rate of fluoride

attachment to vacant and active sites due to interference or repulsion [30]. Additionally, the results showed that increasing the temperature from 20 to 240 minutes significantly improved the adsorption capacity, leading to an efficiency increase of 46.72% to 94.92% or 0.367 mg/g and 0.745 mg/g, respectively. A similar effect of time on the adsorption process was observed in the study done by Jeyaseelan et al. [10], indicating that temperature plays a crucial role in enhancing adsorption capacity and fluoride removal efficiency.

3.2.8. Effect of ionic strength

To investigate the impact of ionic strength on fluoride adsorption using WR@KN, diverse solutions of NaCl and KCl were prepared with varying concentrations of 0.1, 0.2, 0.3, 0.4, and 0.5 moles to assess the adsorption of fluoride in relation to the constituent ions in the solution. Each solution of 4 mL, having a C_i of 5.5 mg/L, was mixed with 0.7 g of WR@KN and optimized factors in 100 ml beakers. Results presented in **Figure 5b** indicate that the increase in NaCl and KCl concentration corresponded with an increase in fluoride removal. This is attributed to the capture of fluoride ions on the surface of the WR@KN by sodium and potassium ions. A 0.3 moles concentration of NaCl was found to have the highest fluoride removal at 97.63%, and a 0.4 moles concentration of KCl showed a fluoride removal of 96.07%, with adsorption capacities of 0.767 and 0.754 mg/g, respectively. In solutions containing increased concentrations of 0.4 and 0.5 moles of NaCl, as well as in the solution containing 0.5 moles of KCl, there was a decrease in fluoride removal, which may be due to the electrostatic repulsion of Cl^- and F^- ions [40]. It was observed that the increase in positively charged ions in the adsorption process enhanced fluoride removal [41], with NaCl being the most effective ion in this experiment.

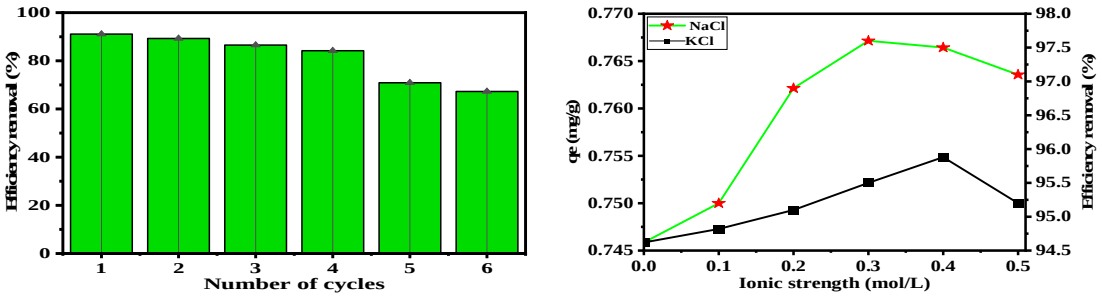

(a) (b)

Figure 5. a) Regeneration of adsorbent, b) Effect of ionic strength on F adsorption.

3.3. Adsorption kinetic models

The present study assessed adsorption kinetics using a C_i of 5.5 mg/L and 0.7 g/100 mL for various time intervals ranging from 20 to 280 minutes. Kinetic data was evaluated using the PFO r and PSO models, as presented in **Figures 6a,** and **6b,** respectively. The kinetic parameters of fluoride adsorption on WR@KN were determined via the corresponding equation. The slope and intercept were obtained by plotting ln (qe-qt) versus time for the PFO model, and t/qt versus time for the PSO model. The results summarized in **Table 2** demonstrate that the pseudo-second-order kinetic model is more suitable than the PFO kinetic model, as evidenced by the observed coefficient of correlation (R^2) which was higher at 0.99984, and an adsorption capacity of 0.754 mg/g, which is in proximity to the experimental value of 0.745 mg/g. These findings align with previous research by Nabbou et al. [29]. Such kinetic data may assist in establishing an effective method for creating a treatment facility for water containing high concentrations of fluoride.

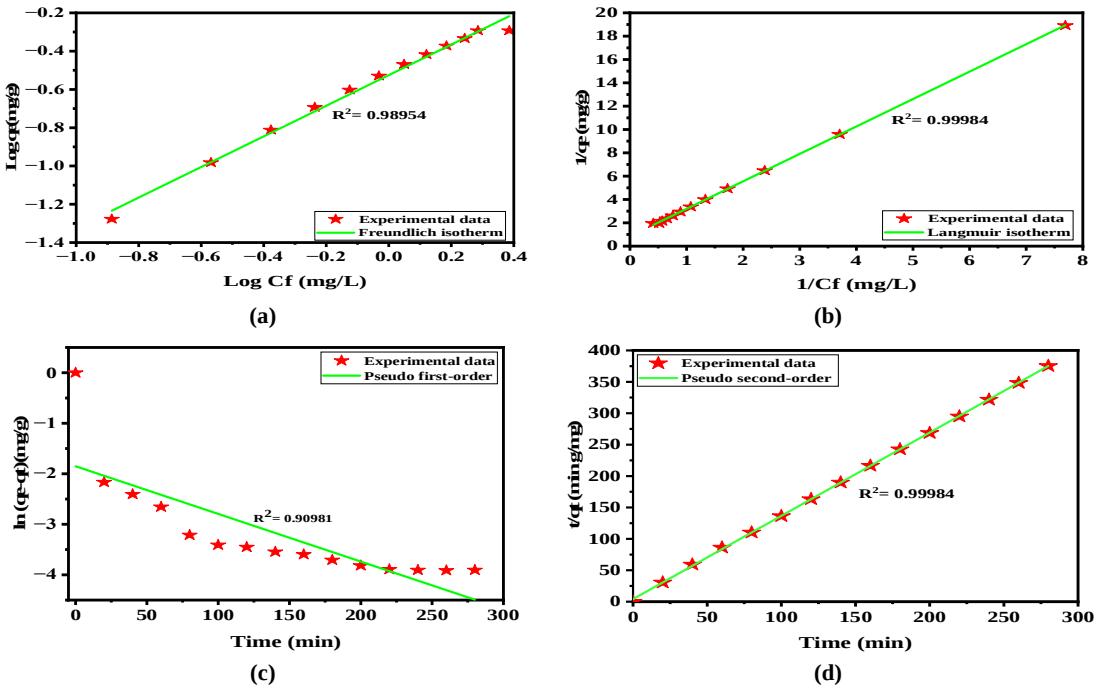

Figure 6. Adsorption kinetics and isotherm plots of fluoride; (a) PFO (b) PSO; (c) Langmuir model, (d) Freundlich model.

3.4. Adsorption isotherm models

The equilibrium isotherm (Langmuir, and Freundlich) was carried out at 25°C with a C_i of 5.5 mg/L and an adsorbent dose of 0.7 g/100 mL. The adsorption isotherm data and fluoride parameters were calculated from the slope and intercept plotted with the corresponding equation, as summarized in **Table 3**. The Langmuir isotherm model was found to be the best fit for fluoride adsorption on WR@KN with a high R^2 value of 0.99984, **Figure 6c**, indicating the favorable adsorption process. The Freundlich isotherm model revealed that the WR@KN has extremely heterogeneous active sites on its surface, with more active sites potentially available at high equilibrium concentrations. The value of 1/n was equal to 0.79938, and the correlation coefficient R^2 was 0.98954, **Figure 6d**, which indicates a high level of heterogeneity at the active sites.

Table 2. Kinetic models for WR@KN.

PFO	PSO
k_1 (min^{-1}) = -3.36786E-05	k_2 (g/mg.min) = 0.138427
q_e (mg/g) = 0.15702818	q_e (mg/g) = 0.754244511
R^2 = 0.90981	R^2 = 0.99984

Table 3. Isotherm models for WR@KN.

Freundlich	Langmuir
K_L = 0.298181	K_L (L/mg) = 0.362313
1/n = 0.79938	R^2 = 0.99984
R^2 = 0.98954	R_L = 0.334

Table 4. Thermodynamic adsorption parameters.

Temperature (°C)	ΔG (kJ/mol)	ΔH (kJ/mol)	ΔS (J/kmol)
24	1.91671395	-77.08253184	-265.3191948
34	4.499283916		

3.5. Thermodynamics

The thermodynamic analysis was conducted at 2 different temperatures, 24 and 34 °C, employing an adsorbent dosage of 0.3 g/100 ml and a C_i of 5 mg/L. **Table 4** displays the values of ΔG°, ΔH°, and ΔS°. The outcomes demonstrate that an upsurge in temperature results in a positive ΔG° (1.91 and 4.49 kJ/mol), indicating that the adsorption of fluoride ions on WR@KN is a spontaneous process. The reaction is exothermic, as implied by the negative value of ΔH° (- 77.08 kJ/mol). Hence, a decrease in temperature amplifies the adsorption of fluoride. Moreover, the negative ΔS° (-256.32 J/kmol) depicts an increase in the irregularity of the solid-liquid interface during fluoride adsorption. These findings are consistent with those obtained by Bhan et al. [37] in their investigation of fluoride removal from water using lanthanum-modified clay soil.

3.6. Comparison of different adsorbents

The efficacy of fluoride removal using WR@KN adsorbent and its associated factors influencing the adsorption mechanism was compared with other reported adsorbents as indicated in **Table 5**. From the presented table, WR@KN successfully removed fluoride ions from 5.5 to 0.28 mg/L at optimum conditions, which is below the WHO-set maximum limit of 1.5 mg/L for fluoride concentration in drinking water.

Table 5. Adsorbent's efficient removal of fluoride with optimum factors.

Adsorbents	Co (mg/l)	pH	Dose (g/l)	Time (hrs.)	Mixing (rpm)	T (°C)	Efficiency (%)	References
Activated kaolin	15	5	12	1	-	60	> 95	[33]
Clay (montmorillonite)	4.5	2.8-6.8	1	>1/2	150	-	66.7	[25]
Clay	5	5.8	10	2		28 ± 2	> 95	[29]
Lateritic soil	2.5	8	4	1/2	300	23 ± 1	30	[42]
Zeolite	5	8.5	100	20	-	-	87	[43]
Micron zirconia/zeolite	5	6	~ 0.14	8	150	25	94.89	[44]
WR@KN	5.5	6	7	3	210	24	94.92	This study

3.7. Recycling of WR@KN

The recycling of adsorbents is paramount from both a financial and ecological standpoint. Regenerated adsorbents can be utilized multiple times. The most challenging aspect of extensive adsorption processes lies in the disposal of adsorbents. The regeneration investigation was conducted using optimized factors. According to the results presented in **Figure 5a**, all adsorbent materials are capable of effectively eliminating fluoride ions for up to the fourth cycle. Through repeated regeneration, the adsorbent's de-fluoridation capability is reduced from 0.715 to 0.528 mg/g, equivalent to 91.09% and 67.27% fluoride removal for the sixth reuse cycle of WR@KN. It has been ascertained that the use of rejuvenated WR@KN for fluoride removal is at its peak during the first four cycles and then declines significantly for the fifth and sixth. This suggests that reusing the prepared adsorbent for de-fluoridation is most effective up to the fourth cycle [33].

4. Conclusions

This study presents a new adsorbent material, which is widely available to purify fluoride from groundwater. The use of WR@KN has been found to be effective and economical for removing fluoride from water sources. The WR@KN was characterized using various analytical techniques (FTIR, XRD, and SEM). Physical and chemical activation methods were applied to improve the adsorption capacity by removing impurities from the surface of the WR@KN. The WR@KN has a pHpzc of 6.7 and mainly comprises oxygen, silicon, and aluminum. The study found that several factors affected the fluoride elimination rate, and the optimum fluoride removal efficiency was achieved under specific conditions. The optimum adsorption capacity of WR@KN is 0.745 mg/g at pH 6, a particle size of 10 µm, a mixing speed of 210 rpm, a temperature of 24 °C, a C_i of 5.5 mg/L, a dose of 0.7 g activated WR@KN, and a contact period of 240 minutes. WR@KN successfully removed fluoride ions from 5.5 to 0.28 mg/L. The Langmuir isotherm model provided the best fit for the fluoride adsorption measurements, indicating that the adsorbent surface has equivalent active sites. The kinetic data obtained using the PSO model were consistent with the experimental values, and the exothermic nature of the fluoride adsorption process was confirmed by a negative ΔH° value. The study demonstrated that WR@KN

can be a cost-effective material for removing fluoride from groundwater.

Acknowledgment

The author is grateful to the Department of Civil Engineering, Chandigarh University for their assistance with the research.

References

[1]. Issabayeva, G, Wong, S.H, Pang, C.Y, Wong, M.C, and Aroua, M.K. (2022). Fluoride removal by low-cost palm shell activated carbon modified with prawn shell chitosan adsorbents. Int. J. Environ. Sci. Technol. 19 (5): 3731–3740.

[2]. Choi, M. Y, Lee, C. G, and Park, S. J. (2022). Conversion of Organic Waste to Novel Adsorbent for Fluoride Removal: Efficacy and Mechanism of Fluoride Adsorption by Calcined Venerupis philippinarum Shells. Water. Air. Soil Pollut. 233(7).

[3]. Wan, K. Huang, L. Yan, J. Ma, B, Huang, X, Luo, Z, Zhang, H, and Xiao, T. (2021). Removal of fluoride from industrial wastewater by using different adsorbents: A review. Sci. Total Environ. 773: 145535.

[4]. Gasparotto, J. M. Roth, D. Perilli, A. L, de O. Franco, D. S. P. Carissimi, E. Foletto, E. L. Jahn, S. L, and Dotto, G. L. (2021). A novel Fe-Al-La trioxide composite: Synthesis, characterization, and application for fluoride ions removal from the water supply. J. Environ. Chem. Eng. 9 (6): 106350.

[5]. Yousefi, M, Yaseri, M, Nabizadeh, R, Hooshmand, E, Jalilzadeh, M, Mahvi, A. H, and Mohammadi, A. A. (2018). Association of Hypertension, Body Mass Index, and Waist Circumference with Fluoride Intake; Water Drinking in Residents of Fluoride Endemic Areas, Iran. Biol. Trace Elem. Res. 185 (2): 282–288.

[6]. KheradPisheh, Z, Mirzaei, M, Mahvi, A. H, Mokhtari, M, Azizi, R. Fallahzadeh, H, and Ehrampoush, M. H. (2018). Impact of drinking water fluoride on human thyroid hormones: A case-control study. Sci. Rep. 8 (1): 1–7.

[7]. Mohammadi, A.A, Yousefi, M, Yaseri, M. Jalilzadeh, M, and Mahvi, A. H. (2017). Skeletal fluorosis in relation to drinking water in rural areas of West Azerbaijan, Iran. Sci. Rep. 7 (1): 4–10.

[8]. Yousefi, M, Ghoochani, M, and Hossein Mahvi, A. (2018). Health risk assessment to fluoride in drinking water of rural residents living in the Poldasht city, Northwest of Iran. Ecotoxicol. Environ. Saf. 148 (October 2017): 426–430.

[9]. Vithanage, M. and Bhattacharya, P. (2015). Fluoride in the environment: sources, distribution and defluoridation. Environ. Chem. Lett. 13 (2): 131–147.

[10]. Jeyaseelan, A, Aswin Kumar, I. Naushad, M, and Viswanathan, N. (2022). Fabrication of hydroxyapatite embedded cerium-organic frameworks for fluoride capture from water. J. Mol. Liq. 354 (September): 118830.

[11]. Kashyap, S.J, Sankannavar, R, and Madhu, G.M. (2021). Fluoride sources, toxicity and fluorosis management techniques – A brief review. J. Hazard. Mater. Lett. 2: 100033.

[12]. Rusiniak, P, Sekuła, K, Sracek, O, and Stopa, P. (2021). Fluoride ions in groundwater of the Turkana County, Kenya, East Africa. Acta Geochim. 40 (6): 945–960.

[13]. Patrick, M. and Sahu, O. (2023). Origins , Mechanisms, and Remedies of Fluoride Ions from Ground and Surface Water : A Review. Chem. Africa. (0123456789).

[14]. Lacson, C.F.Z, Lu, M. C, and Huang, Y.H. (2022). Calcium-based seeded precipitation for simultaneous removal of fluoride and phosphate: Its optimization using BBD-RSM and defluoridation mechanism. J. Water Process Eng. 47: 102658.

[15]. Gangani, N, Joshi, V.C, Sharma, S, and Bhattacharya, A. (2022). Fluoride contamination in water: Remediation strategies through membranes. Groundw. Sustain. Dev. 17 (March).

[16]. Qiu, Y, Ren, L.F, Shao, J, Xia, L, and Zhao, Y. (2022). An integrated separation technology for high fluoride-containing wastewater treatment: Fluoride removal, membrane fouling behavior and control. J. Clean. Prod. 349: 131225.

[17]. Yang, L, Xu, X, Wang, H, Yan, J, Zhou, X, Ren, N, Lee, D.J, and Chen, C. (2022). Biological treatment of refractory pollutants in industrial wastewaters under aerobic or anaerobic condition: Batch tests and associated microbial community analysis. Bioresour. Technol. Reports. 17 (December 2021): 100927.

[18]. Xiang, Y, Xu, H, Li, C, Demissie, H, Qu, S, Luo, J, Jiao, R, and Liu, Y. (2022). Impact of M. aeruginosa on fluoride removal efficiency of AlCl3 and FeCl3 coagulants and the mechanism. J. Environ. Chem. Eng. 10(3): 107691.

[19]. Odabaşı, Ç, Dologlu, P, Gülmez, F, Kuşoğlu, G, and Çağlar, Ö. (2022). Investigation of the factors affecting reverse osmosis membrane performance using machine-learning techniques. Comput. Chem. Eng. 159: 107669.

[20]. Ketharani, J, Hansima, M.A.C.K, Indika, S, Samarajeewa, D.R, Makehelwala, M, Jinadasa, K.B.S.N, Weragoda, S. K, Rathnayake, R.M.L.D, Nanayakkara, K.G.N, Wei, Y, Schensul, S.L, and Weerasooriya, R. (2022). A comparative study of community reverse osmosis and nanofiltration systems for total hardness removal in groundwater. Groundw. Sustain. Dev. 18: 100800.

[21]. Tanvi Newaz, M, Ershadi, M, Carothers, L, Jefferies, M, and Davis, P. (2022). A review and assessment of technologies for addressing the risk of falling from height on construction sites. Saf. Sci. 147: 105618.

[22]. Mousazadeh, M, Alizadeh, S. M, Frontistis, Z, Kabdaşlı, I, Karamati Niaragh, E, Al Qodah, Z, Naghdali, Z, Mahmoud, A. E. D, Sandoval, M. A, Butler, E, and Emamjomeh, M. M. (2021). La electrocoagulación como tecnología prometedora de desfluoración del agua: una revisión del estado del arte de los mecanismos de eliminación y las tendencias de rendimiento. Water

(Switzerland). 13(5).

[23]. Wei, H, Yi, M, Li, X, Shao, L, Gao, F, Cui, X, and Wang, K. (2023). Preparation of metakaolin-based geopolymer microspheres (MK@GMs) and efficient adsorption of F- from acidic wastewater. Sep. Purif. Technol. 310: 123159.

[24]. Pfeifer, A. and Škerget, M. (2020). A review: a comparison of different adsorbents for removal of Cr(VI), Cd(II), and Ni(II). Turkish J. Chem. 44(4): 859–883.

[25]. Diop, S.N. Dieme, M. M, Diallo, M.A, and Diawara, C.K. (2022). Fluoride Excess Removal from Brackish Drinking Water in Senegal by Using KSF and K10 Montmorillonite Clays. J. Water Resour. Prot. 14(01): 21–34.

[26]. Alhassan, S. I, He, Y, Huang, L. Wu, B, Yan, L. Deng, H, and Wang, H. (2020). A review on fluoride adsorption using modified bauxite: Surface modification and sorption mechanisms perspectives. J. Environ. Chem. Eng. 8(6): 104532.

[27]. Kumari, U, Siddiqi, H, Bal, M, and Meikap, B.C. (2020). Calcium and zirconium modified acid activated alumina for adsorptive removal of fluoride: Performance evaluation, kinetics, isotherm, characterization and industrial wastewater treatment. Adv. Powder Technol. 31(5): 2045–2060.

[28]. Gai, W.Z. and Deng, Z.Y. (2021). A comprehensive review of adsorbents for fluoride removal from water: Performance, water quality assessment and mechanism. Environ. Sci. Water Res. Technol. 7(8): 1362–1386.

[29]. Nabbou, N, Belhachemi, M, Boumelik, M, Merzougui, T, Lahcene, D, Harek, Y, Zorpas, A. A, and Jeguirim, M. (2019). Removal of fluoride from groundwater using natural clay (kaolinite): Optimization of adsorption conditions. Comptes Rendus Chim. 22(2–3): 105–112.

[30]. Mondal, N. K, Bhaumik, R, and Datta, J. K. (2015). Removal of fluoride by aluminum impregnated coconut fiber from synthetic fluoride solution and natural water. Alexandria Eng. J. 54(4): 1273–1284.

[31]. Saikia, J. and Goswamee, R.L. (2019). Use of carbon coated ceramic barriers for adsorptive removal of fluoride and permanent immobilization of the spent adsorbent barriers. SN Appl. Sci. 1(6): 1–11.

[32]. Dhanasekaran, P. and Sahu, O. (2021). Arsenate and fluoride removal from groundwater by sawdust impregnated ferric hydroxide and activated alumina (SFAA). Groundw. Sustain. Dev. 12: 100490.

[33]. Ayalew, A.A. (2023). Comparative adsorptive performance of adsorbents developed from kaolin clay and limestone for de-fluoridation of groundwater. South African J. Chem. Eng. 44 (October 2022): 1–13.

[34]. Al-Ghouti, M.A. and Al-Absi, R.S. (2020). Mechanistic understanding of the adsorption and thermodynamic aspects of cationic methylene blue dye onto cellulosic olive stones biomass from wastewater. Sci. Rep. 10(1): 1–18.

[35]. Mahdi, B. A. and Jaafar, R. S. (2020). The ability of Corn waste products to adsorb lead ions from the industrial wastewater. Marsh Bull. 15(1): 19–28.

[36]. Sharma, P.P, Yadav, V, Maru, P. D, Makwana, B. S, Sharma, S, and Kulshrestha, V. (2018). Mitigation of Fluoride from Brackish Water via Electrodialysis: An Environmentally Friendly Process. ChemistrySelect. 3(2): 779–784.

[37]. Bhan, C, Singh, J, Sharma, Y.C, and Koduru, J.R. (2022). Synthesis of lanthanum-modified clay soil-based adsorbent for the fluoride removal from an aqueous solution and groundwater through batch and column process: mechanism and kinetics. Environ. Earth Sci. 81(9).

[38]. Senewirathna, D.S.G.D, Thuraisingam, S, Prabagar, S, and Prabagar, J. (2022). Fluoride removal in drinking water using activated carbon prepared from palmyrah (Borassus flabellifer) nut shells. Curr. Res. Green Sustain. Chem. 5 (March): 100304.

[39]. Jeyaseelan, A, Mezni, A, and Viswanathan, N. (2022). Facile hydrothermal fabrication of functionalized multi-layer graphene oxide encapsulated chitosan beads for enriched fluoride adsorption. J. Appl. Polym. Sci. 139(9).

[40]. Tang, Y, Guan, X, Wang, J, Gao, N, McPhail, M.R, and Chusuei, C.C. (2009). Fluoride adsorption onto granular ferric hydroxide: Effects of ionic strength, pH, surface loading, and major co-existing anions. J. Hazard. Mater. 171(1–3): 774–779.

[41]. Babaeivelni, K. and Khodadoust, A.P. (2013). Adsorption of fluoride onto crystalline titanium dioxide: Effect of pH, ionic strength, and co-existing ions. J. Colloid Interface Sci. 394(1): 419–427.

[42]. Iriel, A, Bruneel, S.P, Schenone, N, and Cirelli, A.F. (2018). The removal of fluoride from aqueous solution by a lateritic soil adsorption: Kinetic and equilibrium studies. Ecotoxicol. Environ. Saf. 149 (June 2017): 166–172.

[43]. Gómez-Hortigüela, L, Pérez-Pariente, J, García, R, Chebude, Y, and Díaz, I. (2013). Natural zeolites from Ethiopia for elimination of fluoride from drinking water. Sep. Purif. Technol. 120: 224–229.

[44]. Gao, Y, Li, M, Ru, Y, and Fu, J. (2021). Fluoride removal from water by using micron zirconia/zeolite molecular sieve: Characterization and mechanism. Groundw. Sustain. Dev. 13(February): 100567.

کارایی جاذب مبتنی بر خاک رس در حذف فلوراید از آب‌های زیرزمینی: فرآیند جذب

موحیزی پاتریک

گروه مهندسی عمران، داشگاه دانشگاه UIE Chandigarh، موحالی، هند

ارسال 2023/04/08، پذیرش 2023/06/16

* نویسنده مسئول مکاتبات: mupax49@gmail.com

چکیده:

دسته‌ای، با حداکثر ظرفیت جذب 0,745 میلی‌گرم بر گرم در pH 6، اندازه ذرات 10 میکرومتر، سرعت اختلاط 210 دور در دقیقه، دمای 24 درجه سانتی‌گراد، دمای اولیه تعیین می‌شود. غلظت فلوراید 5,5 میلی گرم در لیتر، دوز 0,7 گرم WR@KN فعال و دوره تماس 240 دقیقه. WR@KN با موفقیت یون های فلوراید را از 5,5 تا 0,28 میلی گرم در لیتر حذف می‌کند. مدل ایزوترم لانگمویر برای توصیف رفتار جذب فلوراید روی سطح WR@KN با R2 0/99984 مناسب‌ترین است. مدل‌سازی جنبشی جذب نشان می‌دهد که مدل شبه مرتبه دوم بهترین تناسب با 740 mg/g است که نشان می‌دهد فرآیند جذب فلوراید جذب شیمیایی است. ماهیت گرمازایی فرآیند جذب فلوراید با مقدار منفی ΔH° (-77,08) تایید می‌شود. جاذب بازسازی‌شده WR@KN می‌توانست فلوراید را به‌طور موثر برای چهار چرخه اول حذف کند، اما عملکرد آن در چرخه‌های بعدی بدتر شد. افزایش قدرت یونی راندمان حذف فلوراید را افزایش می‌دهد. به طور کلی، نتایج نشان می دهد که جاذب WR@KN می‌تواند یک ماده امیدوارکننده برای حذف مقرون به‌صرفه فلوراید از آب‌های زیرزمینی باشد.

کلمات کلیدی: جاذب، خاک رس سرامیکی، آب آشامیدنی، حذف فلوراید، فن آوری اصلاح.